

Lecture 34

Scattering of Electromagnetic Field

The scattering of electromagnetic field is an important and fascinating topic. It especially enriches our understanding of the interaction of light wave with matter. The wavelength of visible light is several hundred nanometers, with atoms and molecules ranging from nano-meters onward, light-matter interaction is richly endowed with interesting physical phenomena! A source radiates a field, and ultimately, in the far field of the source, the field resembles a spherical wave which in turn resembles a plane wave. When a plane wave impinges on an object or a scatterer, the energy carried by the plane wave is deflected to other directions which is the process of scattering. In the optical regime, the scattered light allows us to see objects, as well as admire all hues and colors that are observed of objects. In microwave, the scatterers cause the loss of energy carried by a plane wave. A proper understanding of scattering theory allows us to understand many physical phenomena around us. We will begin by studying Rayleigh scattering, which is scattering by small objects compared to wavelength. With Rayleigh scattering of a simple sphere, we can understand why the sky is blue and the sunset is red!

34.1 Rayleigh Scattering

Rayleigh scattering is a solution to the scattering of light by small particles. These particles are assumed to be much smaller than wavelength of light. The size of water molecule is about 0.25 nm, while the wavelength of blue light is about 500 nm. Then a simple solution can be found by using quasi-static analysis in the vicinity of the small particle. This simple scattering solution can be used to explain a number of physical phenomena in nature (see Figure 34.1). For instance, why the sky is blue, the sunset so magnificently beautiful, how birds and insects can navigate themselves without the help of a compass. By the same token, it can also be used to explain why the Vikings, as a seafaring people, could cross the Atlantic Ocean over to Iceland without the help of a magnetic compass as the Chinese did in ancient times.



Figure 34.1: The magnificent beauty of nature can be partly explained by Rayleigh scattering [210,211].

When a ray of light impinges on an object, we model the incident light as a plane electromagnetic wave (see Figure 34.2). Without loss of generality, we can assume that the electromagnetic wave is polarized in the z direction and propagating in the x direction. We assume the particle to be a small spherical particle with permittivity ϵ_s and radius a . Essentially, the particle sees a constant field as the plane wave impinges on it. In other words, the particle feels an quasi-electrostatic field in the incident field. The incident field polarizes the particle, making it radiate like a Hertzian dipole. This is the gist of a scattering process: an incident field induces current (in this case, polarization current) on the scatterer. With the induced current, the scatterer re-radiates (or scatters).

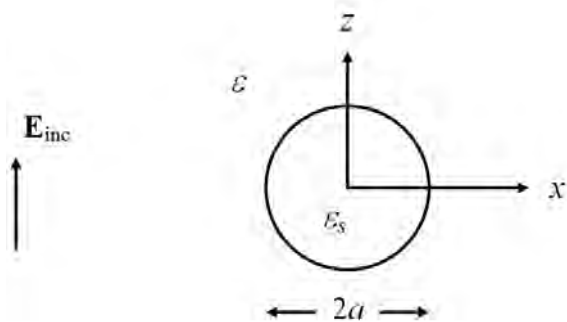


Figure 34.2: Geometry for studying the Rayleigh scattering problem.

34.1.1 Scattering by a Small Spherical Particle

The incident field polarizes the particle making it look like an electric dipole. Since the incident field is time harmonic, the small electric dipole will oscillate and radiate like a Hertzian dipole in the far field. First, we will look at the solution in the vicinity of the scatterer, namely, in the near field. Then we will motivate the form of the solution in the far field of the scatterer. (Solving a boundary value problem by looking at the solutions in two different physical regimes, and then matching the solutions together is known as asymptotic matching.)

A Hertzian dipole can be approximated by a small current source so that

$$\mathbf{J}(\mathbf{r}) = \hat{z}Il\delta(\mathbf{r}) \quad (34.1.1)$$

Without loss of generality, we have assumed the Hertzian dipole to be at the origin. In the above, we can let the time-harmonic current $I = dq/dt = j\omega q$, then

$$Il = j\omega ql = j\omega p \quad (34.1.2)$$

where the dipole moment $p = ql$. The vector potential \mathbf{A} due to a Hertzian dipole, after substituting (34.1.1), is

$$\begin{aligned} \mathbf{A}(\mathbf{r}) &= \frac{\mu}{4\pi} \iiint_V d\mathbf{r}' \frac{\mathbf{J}(\mathbf{r}')}{|\mathbf{r} - \mathbf{r}'|} e^{-j\beta|\mathbf{r} - \mathbf{r}'|} \\ &= \hat{z} \frac{\mu Il}{4\pi r} e^{-j\beta r} = \hat{z} \frac{j\omega\mu ql}{4\pi r} e^{-j\beta r} \end{aligned} \quad (34.1.3)$$

where we have made use of the sifting property of the delta function in (34.1.1) when it is substituted into the above integral.

Near Field

The above gives the vector potential \mathbf{A} due to a Hertzian dipole. Since the dipole is infinitesimally small, the above solution is both valid in the near field as well as the far field. Since the dipole moment ql is induced by the incident field, we need to relate ql to the amplitude of the incident electric field. To this end, we need to convert the above vector potential field to the near electric field of a small dipole.

From prior knowledge, we know that the electric field is given by $\mathbf{E} = -j\omega\mathbf{A} - \nabla\Phi$. From dimensional analysis, the scalar potential term dominates over the vector potential term in the near field of the scatterer. Hence, we need to derive, for the corresponding scalar potential, the approximate solution.

The scalar potential $\Phi(\mathbf{r})$ is obtained from the Lorenz gauge (see (23.2.23)) that $\nabla \cdot \mathbf{A} = -j\omega\mu\epsilon\Phi$. Therefore,

$$\Phi(\mathbf{r}) = \frac{-1}{j\omega\mu\epsilon} \nabla \cdot \mathbf{A} = -\frac{Il}{j\omega\epsilon 4\pi} \frac{\partial}{\partial z} \frac{1}{r} e^{-j\beta r} \quad (34.1.4)$$

When we are close to the dipole, by assuming that $\beta r \ll 1$, we can use a quasi-static approximation about the potential.¹ Then

$$\frac{\partial}{\partial z} \frac{1}{r} e^{-j\beta r} \approx \frac{\partial}{\partial z} \frac{1}{r} = \frac{\partial r}{\partial z} \frac{\partial}{\partial r} \frac{1}{r} = -\frac{z}{r} \frac{1}{r^2} \quad (34.1.5)$$

or after using that $z/r = \cos \theta$,

$$\Phi(\mathbf{r}) \approx \frac{ql}{4\pi\epsilon r^2} \cos \theta \quad (34.1.6)$$

which is the static dipole potential because we are in the near field of the dipole. This dipole induced in the small particle is formed in response to the incident field and its dipole potential given by the previous expression. In other words, the incident field polarizes the small particle into a small dipole.

The incident field can be approximated by a constant local static electric field,

$$\mathbf{E}_{inc} = \hat{z}E_i \quad (34.1.7)$$

This is the field that will polarize the small particle. It can also be an electric field between two parallel plates. The corresponding electrostatic potential for the incident field is then

$$\Phi_{inc} = -zE_i \quad (34.1.8)$$

so that $\mathbf{E}_{inc} \approx -\nabla\Phi_{inc} = \hat{z}E_i$, as $\omega \rightarrow 0$. The scattered dipole potential from the spherical particle in the vicinity of it is quasi-static and is given by

$$\Phi_{sca} = E_s \frac{a^3}{r^2} \cos \theta \quad (34.1.9)$$

which is the potential due to a static dipole. The electrostatic boundary value problem (BVP) has been previously solved and²

$$E_s = \frac{\epsilon_s - \epsilon}{\epsilon_s + 2\epsilon} E_i \quad (34.1.10)$$

Using (34.1.10) in (34.1.9), we get

$$\Phi_{sca} = \frac{\epsilon_s - \epsilon}{\epsilon_s + 2\epsilon} E_i \frac{a^3}{r^2} \cos \theta \quad (34.1.11)$$

On comparing with (34.1.6), one can see that the dipole moment induced by the incident field is that

$$p = ql = 4\pi\epsilon \frac{\epsilon_s - \epsilon}{\epsilon_s + 2\epsilon} a^3 E_i = \alpha E_i \quad (34.1.12)$$

where α is the polarizability of the small particle.

¹This is the same as ignoring retardation effect.

²It was one of the homework problems. See also Section 8.3.6.

Far Field

Now that we have learnt that a small particle is polarized by the incident field, which can be treated as a constant \mathbf{E} field in its vicinity. In other words, the incident field induces a small dipole moment on the small particle. If the incident field is time-harmonic, the the small dipole will be time-oscillating and it will radiate like a time-varying Hertzian dipole whose far field is quite different from its near field (see Section 25.2). In the far field of the Hertzian dipole, we can start with

$$\mathbf{E} = -j\omega\mathbf{A} - \nabla\Phi = -j\omega\mathbf{A} - \frac{1}{j\omega\mu\varepsilon}\nabla\nabla\cdot\mathbf{A} \quad (34.1.13)$$

In the above, Lorenz gauge (see (23.2.23)) has been used to relate Φ to the vector potential \mathbf{A} . But when we are in the far field, \mathbf{A} behaves like a spherical wave which in turn behaves like a local plane wave if one goes far enough. Therefore, $\nabla \rightarrow -j\boldsymbol{\beta} = -j\beta\hat{r}$. Using this approximation in (34.1.13), we arrive at

$$\mathbf{E} \cong -j\omega\left(\mathbf{A} - \frac{\boldsymbol{\beta}\boldsymbol{\beta}}{\beta^2}\cdot\mathbf{A}\right) = -j\omega(\mathbf{A} - \hat{r}\hat{r}\cdot\mathbf{A}) = -j\omega(\hat{\theta}A_\theta + \hat{\phi}A_\phi) \quad (34.1.14)$$

where we have used $\hat{r} = \boldsymbol{\beta}/\beta$. This is similar to the far field result we have derived in Section 26.1.2.

34.1.2 Scattering Cross Section

From (34.1.3), and making use of (34.1.2), we see that $A_\phi = 0$ while

$$A_\theta = -\frac{j\omega\mu ql}{4\pi r}e^{-j\beta r}\sin\theta \quad (34.1.15)$$

Consequently, using (34.1.12) for ql , we have in the far field that³

$$E_\theta \cong -j\omega A_\theta = -\frac{\omega^2\mu ql}{4\pi r}e^{-j\beta r}\sin\theta = -\omega^2\mu\varepsilon\left(\frac{\varepsilon_s - \varepsilon}{\varepsilon_s + 2\varepsilon}\right)\frac{a^3}{r}E_i e^{-j\beta r}\sin\theta \quad (34.1.16)$$

Using local plane-wave approximation that

$$H_\phi \cong \sqrt{\frac{\varepsilon}{\mu}}E_\theta = \frac{1}{\eta}E_\theta \quad (34.1.17)$$

where $\eta = \sqrt{\mu/\varepsilon}$. The time-averaged Poynting vector is given by $\langle\mathbf{S}\rangle = 1/2\Re\{\mathbf{E} \times \mathbf{H}^*\}$. Therefore, the total scattered power is obtained by integrating the power density over a spherical surface when r tends to infinity. Thus, the total scattered power is

$$P_s = \frac{1}{2}\int_0^\pi r^2\sin\theta d\theta \int_0^{2\pi} d\phi E_\theta H_\phi^* = \frac{1}{2\eta}\int_0^\pi r^2\sin\theta d\theta \int_0^{2\pi} d\phi |E_\theta|^2 \quad (34.1.18)$$

$$= \frac{1}{2\eta}\beta^4\left|\frac{\varepsilon_s - \varepsilon}{\varepsilon_s + 2\varepsilon}\right|^2\frac{a^6}{r^2}|E_i|^2 r^2\left(\int_0^\pi \sin^3\theta d\theta\right)2\pi \quad (34.1.19)$$

³The ω^2 dependence of the following function implies that the radiated electric field in the far zone is proportional to the acceleration of the charges on the dipole.

But

$$\begin{aligned} \int_0^\pi \sin^3 \theta d\theta &= - \int_0^\pi \sin^2 \theta d \cos \theta = - \int_0^\pi (1 - \cos^2 \theta) d \cos \theta \\ &= - \int_1^{-1} (1 - x^2) dx = \frac{4}{3} \end{aligned} \quad (34.1.20)$$

Therefore

$$P_s = \frac{4\pi}{3\eta} \left| \frac{\varepsilon_s - \varepsilon}{\varepsilon_s + 2\varepsilon_s} \right|^2 \beta^4 a^6 |E_i|^2 \quad (34.1.21)$$

In the above, even though we have derived the equation using electrostatic theory, it is also valid for complex permittivity defined in Section 7.1.2. One can take the divergence of (7.1.9) to arrive at a Gauss' law for lossy dispersive media, viz., $\nabla \cdot \underline{\varepsilon} \mathbf{E} = 0$ which is homomorphic to the lossless case. Hurrah again to phasor technique!

The scattering cross section is the effective area of a scatterer such that the total scattered power is proportional to the incident power density times the scattering cross section. As such it is defined as

$$\Sigma_s = \frac{P_s}{\langle S_{\text{inc}} \rangle} = \frac{8\pi a^2}{3} \left| \frac{\varepsilon_s - \varepsilon}{\varepsilon_s + 2\varepsilon} \right|^2 (\beta a)^4 \quad (34.1.22)$$

where we have used the local plane-wave approximation that

$$\langle S_{\text{inc}} \rangle = \frac{1}{2\eta} |E_i|^2 \quad (34.1.23)$$

The above also implies that

$$P_s = \langle S_{\text{inc}} \rangle \cdot \Sigma_s$$

In other words, the scattering cross section Σ_s is an effective cross-sectional area of the scatterer that will intercept the incident wave power $\langle S_{\text{inc}} \rangle$ to produce the scattered power P_s .

It is seen that the scattering cross section grows as the fourth power of frequency since $\beta = \omega/c$. The radiated field grows as the second power because it is proportional to the acceleration of the charges on the particle. The higher the frequency, the more the scattered power. This mechanism can be used to explain why the sky is blue. It also can be used to explain why sunset has a brilliant hue of red and orange (see Figure 34.3).

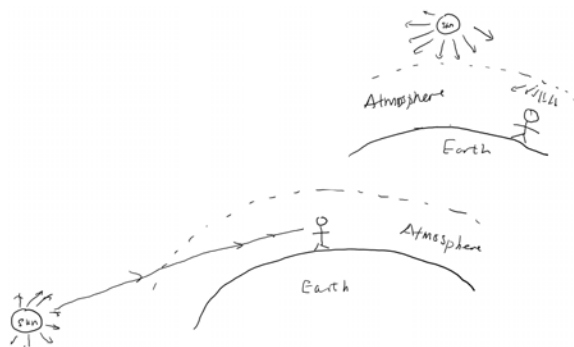


Figure 34.3: During the day time, when we look at the sky, we mainly see scattered sunlight. Since high-frequency light is scattered more, the sky appears blue. At sunset, the sunlight has to go through a thicker atmosphere. Thus, the blue light is scattered away, leaving the red light that reaches the eyes. Hence, the sunset appears red.

The above also explains the brilliant glitter of gold plasmonic nano-particles as discovered by ancient Roman artisans. For gold, the medium resembles a plasma, and hence, we can have $\varepsilon_s < 0$, and the denominator can be very small giving rise to strongly scattered light (see Section 8.3.6).

Furthermore, since the far field scattered power density of this particle is

$$\langle S \rangle = \frac{1}{2\eta} E_\theta H_\phi^* \sim \sin^2 \theta \quad (34.1.24)$$

the scattering pattern of this small particle is not isotropic. In other words, these dipoles radiate predominantly in the broadside direction but not in their end-fire directions. Therefore, insects and sailors can use this to figure out where the sun is even in a cloudy day. In fact, it is like a rainbow: If the sun is rising or setting in the horizon, there will be a bow across the sky where the scattered field is predominantly linearly polarized.⁴ Such a “sunstone” for direction finding is shown in Figure 34.4.

⁴You can go through a Gedanken experiment to convince yourself of such.



Figure 34.4: A sunstone can indicate the polarization of the scattered light. From that, one can deduce where the sun is located (courtesy of Wikipedia).

34.1.3 Small Conductive Particle

The above analysis is for a small dielectric particle. The quasi-static analysis may not be valid for when the conductivity of the particle becomes very large. For instance, for a perfect electric conductor immersed in a time varying electromagnetic field, the magnetic field in the long wavelength limit induces eddy current in PEC sphere.⁵ Hence, in addition to an electric dipole component, a PEC sphere also has a magnetic dipole component. The scattered field due to a tiny PEC sphere is a linear superposition of an electric and magnetic dipole components. These two dipolar components have electric fields that cancel precisely at certain observation angle. It gives rise to deep null in the bi-static radar scattering cross-section (RCS)⁶ of a PEC sphere as illustrated in Figure 34.5.

⁵Note that there is no PEC at optics. A metal behaves more like a plasma medium at optical frequencies.

⁶Scattering cross section in microwave range is called an RCS due to its prevalent use in radar technology.

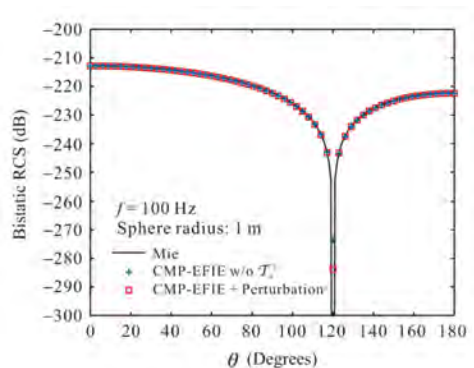


Figure 34.5: RCS (radar scattering cross section) of a small PEC scatterer (courtesy of Sheng et al. [212]).

34.2 Mie Scattering

When the size of the dipole becomes larger compared to wavelength λ , quasi-static approximation is insufficient to approximate the solution. Then one has to solve the boundary value problem in its full glory usually called the full-wave theory or Mie theory [213,214]. With this theory, the scattering cross section does not grow indefinitely with frequency as in (34.1.22). It has to saturate to a value for increasing frequency. For a sphere of radius a , the scattering cross section becomes πa^2 in the high-frequency limit. This physical feature of this plot is shown in Figure 34.6, and it also explains why the sky is not purple.

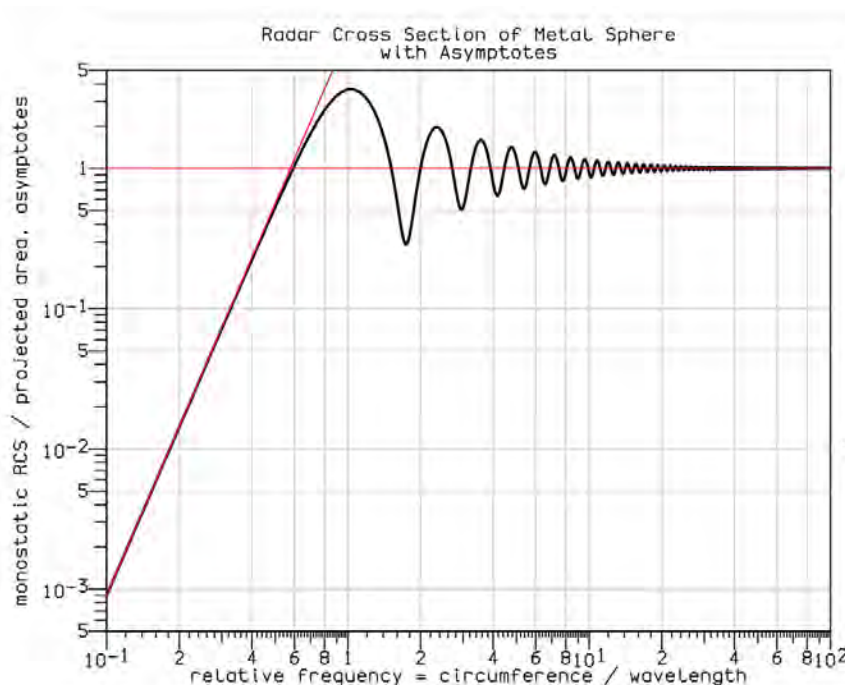


Figure 34.6: Radar cross section (RCS) calculated using Mie scattering theory [214].

34.2.1 Optical Theorem

Before we discuss the Mie scattering solution, let us discuss an amazing theorem called the optical theorem. This theorem says that the scattering cross section of a scatterer depends only on the forward scattering power density of the scatterer. In other words, if a plane wave is incident on a scatterer, the scatterer will scatter the incident power in all directions. But the total power scattered by the object is only dependent on the forward scattering power density of the object or scatterer. This amazing theorem is called the optical theorem, and the proof of this is given in J.D. Jackson's book [48].

The true physical reason for this is power orthogonality. Two plane waves cannot interact or exchange power with each other unless they share the same \mathbf{k} or $\boldsymbol{\beta}$ vector, where $\boldsymbol{\beta}$ is both the plane wave direction of the incident wave as well as the forward scattered wave. This is similar to power orthogonality in a waveguide, and it happens for orthogonal modes in waveguides [83, 178].

The scattering pattern of a scatterer for increasing frequency is shown in Figure 34.7. For Rayleigh scattering where the wavelength is long, the scattered power is distributed isotropically save for the doughnut shape of the radiation pattern, namely, the $\sin^2(\theta)$ dependence. As the frequency increases, the power is scattered increasingly in the forward direction. The reason being that for very short wavelength, the scatterer looks like a disc to the incident

wave, casting a shadow in the forward direction. Hence, there has to be scattered field in the forward direction to cancel the incident wave to cast this shadow.

In a nutshell, the scattering theorem is intuitively obvious for high-frequency scattering. The amazing part about this theorem is that it is true for all frequencies.

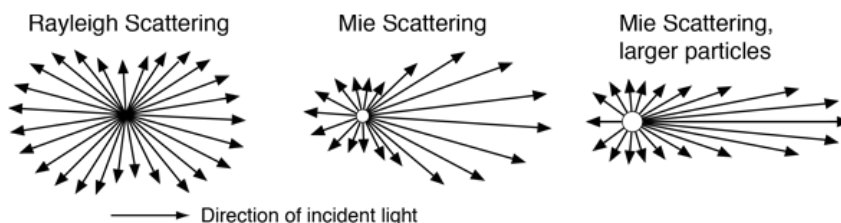


Figure 34.7: A particle scatters increasingly more in the forward direction as the frequency increases (Courtesy of hyperphysics.phy-astr.gsu.edu).

34.2.2 Mie Scattering by Spherical Harmonic Expansions

As mentioned before, as the wavelength becomes shorter, we need to solve the boundary value problem in its full glory without making any approximations. This closed form solution can be found for a sphere scattering by using separation of variables and spherical harmonic expansions that will be discussed in the section.

The Mie scattering solution by a sphere is beyond the scope of this course.⁷ The separation of variables in spherical coordinates is not the only useful for Mie scattering, it is also useful for analyzing spherical cavity. So we will present the precursor knowledge so that you can read further into Mie scattering theory if you need to in the future.

34.2.3 Separation of Variables in Spherical Coordinates⁸

To this end, we look at the scalar wave equation $(\nabla^2 + \beta^2)\Psi(\mathbf{r}) = 0$ in spherical coordinates. A lookup table can be used to evaluate $\nabla \cdot \nabla$, or divergence of a gradient in spherical coordinates. Hence, the Helmholtz wave equation becomes⁹

$$\left(\frac{1}{r^2} \frac{\partial}{\partial r} r^2 \frac{\partial}{\partial r} + \frac{1}{r^2 \sin \theta} \frac{\partial}{\partial \theta} \sin \theta \frac{\partial}{\partial \theta} + \frac{1}{r^2 \sin^2 \theta} \frac{\partial^2}{\partial \phi^2} + \beta^2 \right) \Psi(\mathbf{r}) = 0 \quad (34.2.1)$$

Noting the $\partial^2/\partial\phi^2$ derivative, by using separation of variables technique, we assume $\Psi(\mathbf{r})$ to be of the form

$$\Psi(\mathbf{r}) = F(r, \theta) e^{jm\phi} \quad (34.2.2)$$

⁷But it is treated in J.A. Kong's book [32] and Chapter 3 of W.C. Chew, Waves and Fields in Inhomogeneous Media [35] and many other textbooks [48, 65, 181].

⁸May be skipped on first reading.

⁹By quirk of mathematics, it turns out that the first term on the right-hand side below can be simplified by observing that $\frac{1}{r^2} \frac{\partial}{\partial r} r^2 = \frac{1}{r} \frac{\partial}{\partial r} r$.

This will simplify the $\partial/\partial\phi$ derivative in the partial differential equation since $\frac{\partial^2}{\partial\phi^2}e^{jm\phi} = -m^2e^{jm\phi}$. Then (34.2.1) becomes

$$\left(\frac{1}{r^2}\frac{\partial}{\partial r}r^2\frac{\partial}{\partial r} + \frac{1}{r^2\sin\theta}\frac{\partial}{\partial\theta}\sin\theta\frac{\partial}{\partial\theta} - \frac{m^2}{r^2\sin^2\theta} + \beta^2\right)F(r, \theta) = 0 \quad (34.2.3)$$

Again, by using the separation of variables, and letting further that

$$F(r, \theta) = b_n(\beta r)P_n^m(\cos\theta) \quad (34.2.4)$$

where we require that

$$\left\{\frac{1}{\sin\theta}\frac{d}{d\theta}\sin\theta\frac{d}{d\theta} + \left[n(n+1) - \frac{m^2}{\sin^2\theta}\right]\right\}P_n^m(\cos\theta) = 0 \quad (34.2.5)$$

when $P_n^m(\cos\theta)$ is the associate Legendre polynomial. Note that (34.2.5) is an eigenvalue problem with eigenvalue $n(n+1)$, and $|m| \leq |n|$. The value $n(n+1)$ is also known as separation constant.

Consequently, $b_n(kr)$ in (34.2.4) satisfies

$$\left[\frac{1}{r^2}\frac{d}{dr}r^2\frac{d}{dr} - \frac{n(n+1)}{r^2} + \beta^2\right]b_n(\beta r) = 0 \quad (34.2.6)$$

The above is the spherical Bessel equation where $b_n(\beta r)$ is either the spherical Bessel function $j_n(\beta r)$, spherical Neumann function $n_n(\beta r)$, or the spherical Hankel functions, $h_n^{(1)}(\beta r)$ and $h_n^{(2)}(\beta r)$. The spherical functions are the close cousins of the cylindrical functions. They are related to the cylindrical functions via [35, 49] ¹⁰

$$b_n(\beta r) = \sqrt{\frac{\pi}{2\beta r}}B_{n+\frac{1}{2}}(\beta r) \quad (34.2.7)$$

It is customary to define the spherical harmonic as [48, 110]

$$Y_{nm}(\theta, \phi) = \sqrt{\frac{2n+1}{4\pi}\frac{(n-m)!}{(n+m)!}}P_n^m(\cos\theta)e^{jm\phi} \quad (34.2.8)$$

The above is normalized such that

$$Y_{n,-m}(\theta, \phi) = (-1)^m Y_{nm}^*(\theta, \phi) \quad (34.2.9)$$

and that

$$\int_0^{2\pi} d\phi \int_0^\pi \sin\theta d\theta Y_{n'm'}^*(\theta, \phi)Y_{nm}(\theta, \phi) = \delta_{n'n}\delta_{m'm} \quad (34.2.10)$$

These functions are also complete¹¹ like Fourier series, so that

$$\sum_{n=0}^{\infty} \sum_{m=-n}^n Y_{nm}^*(\theta', \phi')Y_{nm}(\theta, \phi) = \delta(\phi - \phi')\delta(\cos\theta - \cos\theta') \quad (34.2.11)$$

¹⁰By a quirk of nature, the spherical Bessel functions needed for 3D wave equations are in fact simpler than cylindrical Bessel functions needed for 2D wave equation. One can say that 3D is real, but 2D is surreal.

¹¹In a nutshell, a set of basis functions is complete in a subspace if any function in the same subspace can be expanded as a sum of these basis functions.